Synthesis and structural and optical properties of mesoporous silica containing silver nanoparticles

1997 J. Phys.: Condens. Matter 9 7257

(http://iopscience.iop.org/0953-8984/9/34/015)

J. Phys.: Condens. Matter **9** (1997) 7257–7267. Printed in the UK PII: S0953-8984(97)81405-1

Synthesis and structural and optical properties of mesoporous silica containing silver nanoparticles

Cai Weiping and Zhang Lide

Institute of Solid State Physics, Academia Sinica, Hefei, Anhui 230031, People's Republic of China

Received 29 January 1997, in final form 24 March 1997

Abstract. Mesoporous silica with silver (Ag) nanoparticles within its pores was synthesized by thermal decomposition of silver nitrate. The structure of this new material was examined by x-ray diffraction, transmission electron microscope and Brunauer–Emmett–Teller techniques, and its optical absorption spectra were measured. It has been shown that Ag nanoparticles are isolated from each other and highly uniformly dispersed in pores which are less than 8 nm in diameter. The size of Ag particles follows a log-normal distribution function. Ag particle doping leads to a large red shift of the absorption edge and the edge position can be controlled across the whole visible region by varying the amount of Ag doping. There is no surface plasmon resonance peak other than an absorption edge on the absorption spectra. These facts are explained in terms of interband absorption and dipole interaction of Ag particles in silica, and interaction between pore walls and Ag particles.

1. Introduction

During the past decade, spectacular progress has been made in the development of new materials. Among these are nanostructured materials. It is well known that nanometre-sized particles, because of their small size and high specific surface area, display many unique properties [1, 2]; similarly, mesoporous solids, due to their large internal surface area and small pore size, have found great utility [3–5]. If we assemble the nano-scaled particles (semiconductors, compounds or metals) into the pores of mesoporous solids, a new material will be formed. This nanoparticle-loaded porous solid will undoubtedly possess some unique properties of both the nanoparticle and the mesoporous solid. This new material, however, is significantly different from the recently extensively reported glass–metal colloid composites (films), organic–inorganic nanocomposites (films) or other nanocomposite films [6–9]. The large number of pores in the mesoporous solid, of the order of 10^{19} pores g^{-1}, results in a large surface area, in some cases reaching 900 m^2 g^{-1} [10]. Because the pores are small, interactions at the pore–nanoparticle interface are likely to be extensive and may significantly alter the physico-chemical properties of the particles within pores. On the other hand, because all the pores in the porous solids are interconnected and open to the ambient, the nanosized particles located within the pores are also in contact with the ambient air. The nanoparticles within the pores are small in size and chemically active [1, 2]. Therefore, there inevitably exist the interactions between the ambient and the nano-scale phase, especially metal particles. So this new type of composite material will have properties that neither the nanoparticle nor the mesoporous solid possess. For example, the dispersion of semiconductor ultrafine particles in the pores of porous glass produces optical switching

0953-8984/97/347257+11$19.50

and optical nonlinearity effects [11]; polyaniline filaments within the mesoporous channel host (aluminosilicate) have significant conductivity, and this demonstration of conjugated polymer with mobile charge carriers in nanometre channels represents a step toward the design of nanometre electronic devices [12]. Recently, we have synthesized a new material by putting silver (Ag) nanoparticles into the mesoscopic pores of porous silica with help of a new method. In this material the silver nanoparticles are separated and highly uniformly dispersed within the pores of the porous silica; it displays optical switching and memory effects under different ambient conditions [13], a transition from surface adsorption to surface oxidation of Ag particles within pores of silica with variation in ambient conditions [14], and optical features of a semiconductor with direct band gap and ambient-induced interface coupling effect. These results will be reported elsewhere. Here we focus on the synthesis and characterization of Ag-particle-loaded porous silica.

2. Method and quantitative relations

2.1. Method

Several synthetic methods for compound or semiconductor-particle-loaded mesoporous solids have been reported. For example, a pre-formed (semiconductor) colloid may be introduced into the reaction mixture during a sol–gel process [15]; or semiconductor particles may be directly synthesized within the gel pores [16]. Obviously, the resultant properties of the material prepared using these methods are restricted by the wide size distribution of the (semiconductor) particles. In principle, the drawbacks in these methods can be overcome by employing a well defined porous solid of uniform pore diameter and utilizing diffusion of pre-formed particles to achieve the desired result, but it is difficult to make a well defined porous solid with uniform pore diameter and the diffusion of the colloid is also slow. For the synthesis of a nanometre-metal-particle-loaded silica mesoporous solid, we present a method avoiding the drawbacks in the methods above.

Our method is based on the following reaction:

$$\mathrm{AgNO_3} \xrightarrow{>573\ \mathrm{K}} \mathrm{Ag} + \mathrm{NO_2}\uparrow + \tfrac{1}{2}\mathrm{O_2}\uparrow . \tag{1}$$

The pre-formed silica gel (dry or wet gel) is cleaned sufficiently with distilled water before it is soaked in a silver nitrate ($AgNO_3$) solution with a certain concentration. We can also increase the temperature of the soaking solution to shorten the soaking time. Usually, the diffusion of ions in solution is faster than that of colloid. After having been sufficiently soaked, the gel is taken out and dried to remove the solvent in it. Obviously, it is certain that $AgNO_3$ crystallites are present within the pores of the dried soaked gel. Then it is heated in the air to more than 573 K and held at that temperature to let $AgNO_3$ decompose and leave the Ag particles in the pores. This method is naturally suitable for other porous materials (e.g. Ag_2O_3 and TiO_2) as host in addition to silica, and also for other metals as guest if their salts can decompose at a temperature like that for $AgNO_3$. Because the pores of mesoporous solids are small enough in size, possible flow of solution between pores, during drying, can be effectively avoided due to surface tension of solution within pores, and hence we can expect to obtain the mesoporous solid uniformly dispersed with nanoparticles within its pores.

2.2. Control of the loading amount of Ag

If we assume that evaporation of Ag^+ ions during drying for the soaked samples is negligible, which has been justified by weighing the sample before and after doping, the total loading volume of Ag in unit volume of the mesoporous solid V_{Ag} can be expressed as

$$V_{Ag} = PnV_m \tag{2}$$

where P is the porosity of the mesoporous solid (or the total pore volume in unit volume of the porous solid), n the molar concentration of Ag^+ ions in the soaking solution and V_m the molar volume of silver. The loading amount of Ag can also be expressed in weight:

$$W_{Ag} = \frac{P}{1-P}\frac{\rho_{Ag}}{\rho_0}V_m n \tag{3}$$

where W_{Ag} is the weight of Ag in unit weight of the host material and ρ_{Ag} and ρ_0 are the densities of silver and the skeleton of the porous solid respectively. We see that the loading amount of Ag is directly proportional to the concentration n of soaking solution. If P is given, the amount only depends on the value of the parameter n. Hence we can quantitatively control the amount of Ag in the porous material according to (2) or (3).

3. Experimental procedures

3.1. Preparation of samples

The monolithic porous silica was prepared by the sol–gel technique [17, 18]. First tetraethyl orthosilicate, alcohol and distilled water were mixed together in the molar ratio 1:4:20 to make a homogeneous solution. A small amount of water containing nitric acid (HNO_3 solution) was slowly dropped into the solution (until pH = 1) at room temperature (298 K) under stirring over a duration of 20 min followed by another 20 min stirring. The solution was poured into a polytetrafluoroethylene (Teflon) cylinder and sealed with a transparent glue tape to react to form gel at 323 K. After gelation (about 48 h), the gel was aged at 353 K for 7 d. To dry the wet gel thus prepared, the glue tape was perforated with several pinholes of 1 mm diameter and the temperature was raised from 353 to 393 K over 7 d. The dried gel cylinder obtained in this way was crackfree and typically was 25 mm in diameter and 0.5–1.5 mm in thickness. The dried gel was then heated to 1073 K for 1 h in an electric heating furnace (in air) and the monolithic porous silica sample was thus prepared. The final porosity is estimated to be about 50% by the pyconometry technique [19]. The Brunauer–Emmett–Teller (BET) technique (described in section 3.2) shows that the measured value of specific surface area is 654 $m^2\ g^{-1}$ and pore diameters fall into the range of 2–10 nm. Hence silica prepared in this way is a typical mesoporous solid [3]. The pre-formed porous silica samples were then soaked in $AgNO_3$ solutions (0.25, 0.5 and 1.0 M) at room temperature. After they had been sufficiently soaked (20 d or more), the samples were taken out and dried at a temperature from room temperature up to 423 K to remove the solvent from the pores. Then the dried soaked samples were heated in air to 773 K and held for 1 h to let $AgNO_3$ decompose and only leave the silver particles within the pores of the silica. The unloaded sample was also subjected to the same treatment for reference.

3.2. Characterization of samples

The porosity and density for the samples studied (doped and reference samples) were measured by the pyconometry technique [19]. When the loading amount of Ag in silica

is small the doping amount obtained by weighing the sample before and after doping is usually unreliable because there are more OH groups remaining on pore walls after doping (773 K) than before doping (1073 K), but when the amount is large enough a significant decrease in the area of pore wall exposed to air due to the existence of Ag particles will partially cancel out this difference in OH group number, and the weight corresponding to the difference in OH group number is relatively small compared with the doping amount. It is difficult to know the difference in OH group number between before and after doping. Here we assume that the doping amount for the samples studied in this paper is large enough, and ignore the difference between before and after doping in OH group number, and, hence, the doping amount of Ag in silica can be experimentally determined by the weighing method. The value obtained in this way was compared with that obtained from (3). Nitrogen adsorption isotherms were obtained using a gas adsorption apparatus (ASAP 2000). Specific surface areas were evaluated using the BET equation [20], with data points between reduced pressure values of 0.05 and 0.20 and assuming the surface area occupied by one nitrogen molecule to be 16.2 $Å^2$. The measured error of specific surface area can be controlled to below 1.5%.

X-ray diffraction (XRD) measurements were carried out to examine the crystallinity of the samples. For direct observation of Ag particles in silica, the samples were first ground. The powders obtained in this way were dispersed in acetone in a test tube. The latter was placed in an ultrasonic bath for 10 min. The clear liquid from the top portion of the test tube was taken and a few drops of this liquid were placed on a carbon-coated copper grid. After the evaporation of acetone the copper grid was mounted on a JEM 200CX transmission electron microscope (TEM) operated at 200 kV, and hence the microstructure, selected area electron diffraction patterns were investigated. The size and distribution of microcrystals were inspected. The average Ag particle diameter $\overline{d}$ for each doped sample is estimated by the equation

$$\overline{d} = \frac{1}{N}\sum_{i=1}^{n_0} d_i n_i \tag{4}$$

where d_i is the diameter in the ith interval of the histogram, n_i the particle number in the ith interval, n_0 the total number of intervals and

$$N = \sum_{i=1}^{n_0} n_i . \tag{5}$$

The standard deviation of the particle diameter S_d is determined by the formula

$$S_d = \left\{ \frac{1}{N-1}\sum_{j=1}^{N} \left(d_j - \overline{d}\right)^2 \right\}^{1/2} . \tag{6}$$

3.3. Optical measurement

The optical absorption spectra for the planar-like Ag-loaded and reference samples with a thickness of 0.5 mm were measured on a Cary 5E UV–VisNir spectrophotometer over the wavelength range from 1200 to 180 nm (optical scanning starts from long wavelength, 1200 nm, to short wavelength, 180 nm). The measurement was performed immediately after the original annealing at 773 K for 1 h and air-cooling to 298 K.

4. Results and discussion

The amount of Ag in silica obtained by the weighing method is shown in table 1 for the annealed soaked samples studied in this paper. The corresponding W_{Ag} values from (3) are also listed in this table (letting $\rho_0 = 2.2$ g cm^{-3}, $\rho_{Ag} = 10.5$ g cm^{-3}, $V_m = 10.3$ cm^3 mol^{-1} and $P = 0.5$). The theoretical results are in good agreement with measured values.

Table 1. The loading amount of Ag in silica obtained by the weighing method and from (3) for doped samples annealed at 773 K for 1 h.

n (M)	W_{Ag} (wt%) (measured)	W_{Ag} (wt%) (calculated)
0.25	1.1	1.23
0.5	2.3	2.46
1.0	5.0	4.91

4.1. Location of loaded particles

It has been shown that the measured specific surface area decreases significantly from 654 m^2 g^{-1} for the reference sample to, say, for the sample with about 1 wt% Ag, 561 m^2 g^{-1} for the dried soaked state or 587 m^2 g^{-1} for the annealed state although the real specific surface area may increase due to the existence of $AgNO_3$ or Ag particles into the pores. This can be attributed to the presence of particles within the pores of silica, which leads to difficulty for nitrogen molecules in entering too small a free space during measurement and hence the partial area cannot be measured. The presence of the particles within pores is more clearly shown by the nitrogen sorption isotherms for reference, and dried or annealed soaked samples (see figure 1). The slope for the former is larger than those of the latter for relative pressures less than 0.7. At given relative pressure x, the critical radius of a pore for condensing gas into liquid state $r = r_K + t$, where r_K is the Kelvin radius [21] and t the thickness of the sorption layer on the pore wall. In nitrogen sorption, Wheeler gave the expressions [22]

$$\begin{aligned} r_K &= -4.14\big(\log_{10} x\big)^{-1} \\ t &= -5.57\big(\log_{10} x\big)^{-1/3} \end{aligned} \tag{7}$$

where t and r_K are in ångströms. When $x = 0.7$ $r \approx 3.7$ nm. This means that the particles are located within the pores which are less than about 8 nm in diameter. In addition, the isotherm sorption curve for a doped sample with annealing at 773 K for 1 h is located between those of the reference and the dried soaked samples. This should be attributed to the decomposition of $AgNO_3$ crystallites within pores during annealing. Decomposition of $AgNO_3$ within pores leaves only Ag crystallites within the pores of the silica host and hence there is an increase in the free space of pores and the whole isotherm curve rises, but the curve is still lower than that of the undoped sample due to the existence of Ag particles within the pores. XRD has confirmed, in addition to amorphous silica, the presence of crystalline $AgNO_3$ for the dried soaked sample and only crystalline Ag for the annealed doped sample, as shown in figure 2.

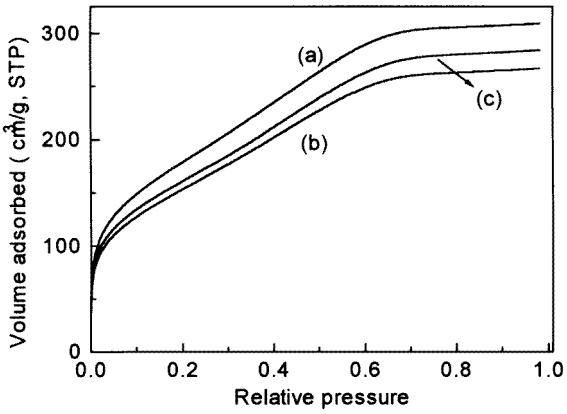

Figure 1. Nitrogen sorption isotherms of undoped sample (a), soaked sample dried at up to 423 K (concentration of soaking solution, 0.25 M, or Ag doping amount, 1.1 wt%) (b) and dried soaked sample (b) followed by annealing at 773 K for 1 h (c).

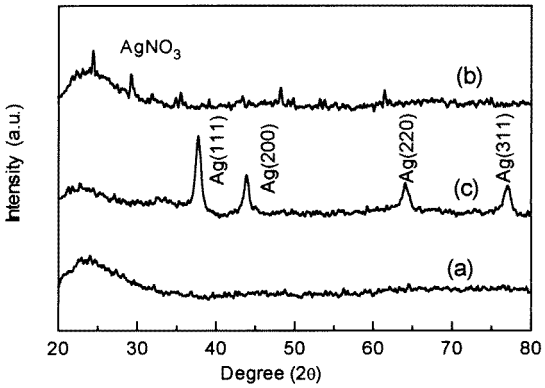

Figure 2. XRD for silica host without doping (a), soaked sample dried at up to 423 K (or sample (b) in figure 1) (b) and sample (b) annealed at 773 K for 1 h (c).

4.2. Size distribution and dispersivity of Ag particles within pores

For verification of complete decomposition of $AgNO_3$ into Ag crystallites, and examination of distribution of the particles within pores for the annealed doped sample, TEM examination was performed. Figure 3(a) is a micrograph for the doped sample containing about 1% Ag. The particles are highly uniformly dispersed in silica. Figure 3(b) is the selected area electron diffraction pattern from the micrograph shown in figure 3(a). The values of interplanar spacings d_{hkl} calculated from the diameters of the diffraction rings are given in table 2. The standard ASTM d_{hkl} values for silver are also listed in this table. The observed data agree with those of bulk silver. There are no other crystallites (including $AgNO_3$) to be found in our TEM examination. Therefore, it is reasonable to suggest that the crystallites within pores of silica are only (or mainly) Ag particles.

4.2.1. Size distribution of Ag particles. The histograms of the silver particle sizes were plotted for all doped samples. They are well fitted by the log-normal distribution function

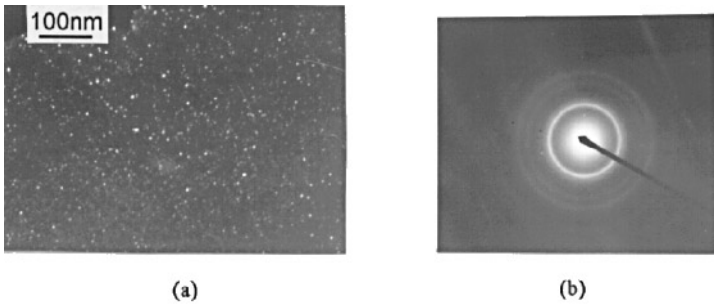

Figure 3. (a) The TEM micrograph of the doped sample annealed at 773 K for 1 h (Ag 1.1 wt%); (b) the electron diffraction pattern of (a).

Table 2. Interplanar spacing d_{khl} values and standard silver (ASTM) data (nm).

Observed	Standard silver
0.2395	0.2359
0.2084	0.2043
0.1468	0.1445
0.1247	0.1231
0.0940	0.0938

given by

$$\Delta n = \frac{1}{\sqrt{2\pi}\ln\sigma}\exp\left\{-\frac{1}{2}\left[\frac{\ln(d/\overline{d})}{\ln\sigma}\right]^2\right\}\Delta(\ln d) \tag{8}$$

where Δn is the fractional number of particles per logarithmic diameter interval $\Delta(\ln d)$, $\overline{d}$ is the average diameter and σ the geometrical standard deviation. Figure 4 shows the histogram of Ag particle size and the fitting curve of the midinterval point of the histogram for the sample with about 1% Ag. The fitting curve is in good agreement with the histogram. The average particle diameter and standard deviation σ-values obtained by a statistical method ((4) and (6)) and by fitting according to the log-normal distribution function (8) are seen in table 3. The sizes of Ag particles for samples annealed at 773 K for 1 h are all less than 5 nm in diameter.

Table 3. The average diameter $\overline{d}$ and standard deviation of doped silver particles.

Doping amount of Ag (wt%)	Log-normal		Statistical method	
	$\overline{d}$ (nm)	σ (nm)	$\overline{d}$ (nm)	S_d (nm)
1.1	2.4	1.4	2.6	1.1
2.3	2.8	1.8	3.0	1.5
5.0	3.6	1.9	3.5	1.8

4.2.2. Dispersivity of Ag particles in silica. It seems, from figure 3(a), that Ag particles are highly uniformly dispersed in the silica matrix. For a quantitative description of dispersivity of Ag particles in silica, the micrograph is first digitized by hand to produce a matrix of ones

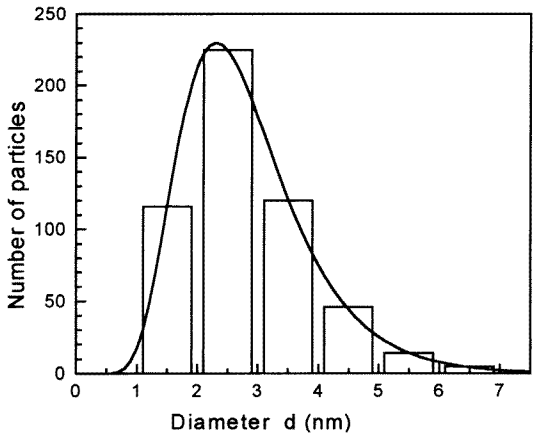

Figure 4. A size distribution histogram of the silver particles in the doped sample shown in figure 3(a); the curve is the corresponding fitting result of the midinterval points of the histogram by the log-normal function.

and blanks corresponding to the presence or absence of a particle, as previously described [23]. Different circles (with different radii) are then chosen in the image and the number N of ones in each circle is counted. N is analysed according to the power law

$$N \propto R^D \tag{9}$$

where R is the radius of the circle chosen and D a constant. Obviously, if Ag particles are uniformly dispersed, D should have a value of two. Significant deviation of the value of D from two means that the distribution of Ag particles is not uniform and becomes one of fractal dimensions [23, 24]. The plots of ln N versus ln R for the samples with different Ag amounts are shown in figure 5. The data points for each sample are least-squares fitted to a line whose slope gives the value of D. It has been shown that the values of D for the samples studied in this paper all fall into the range 2.00 ± 0.05, i.e. around two. The data presented here span only a limited range of R, namely 25–350 nm. Therefore, it is likely that the samples under investigation have Ag particles uniformly dispersed in the silica host over a radius > 25 nm.

Because the pores of silica host are small enough in size and of high dispersivity, the possible flow of solution between adjacent pores during drying for the soaked sample is effectively avoided due to the surface tension of the solution, resulting in uniform dispersion of Ag particles in the silica.

4.3. Optical measurements

Figure 6 shows the optical absorption spectra for undoped and Ag-doped samples. For all Ag-particle-loaded samples with the original annealing treatment (773 K for 1 h), the absorption spectra show only an absorption edge (see curves (b)–(d) in figure 6). There is no surface plasma resonance absorption peak at around 400 nm, in contrast to the Ag–silica system reported in many publications [25–27]. Compared with the reference sample, there exists a large red shift ($\gtrsim$100 nm) for doped samples. The absorption edge shifts from about 185 nm to about 700 nm with increase in Ag loading amount up to 5 wt%. Therefore, the position of the absorption edge can be controlled by the Ag loading amount across the whole visible region, which is undoubtedly of importance.

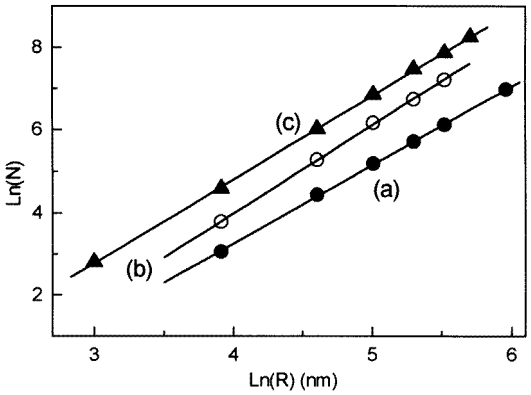

Figure 5. Logarithmic plots of N versus R for the Ag-doped samples with Ag amounts 1.1 wt% (a), 2.3 wt% (b) and 5.0 wt% (c) (N is the number of particles counted in a circular region of radius R).

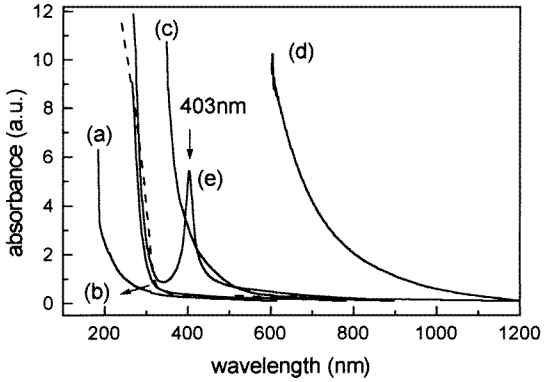

Figure 6. Optical absorption spectra for an undoped sample (a) and doped samples annealed at 773 K for 1 h with Ag amounts 1.1 wt% (b), 2.3 wt% (c) and 5.0 wt% (d). Curve (e) is sample (b) followed by additional annealing at 1073 K for 1 h. The dashed curve is the calculated spectrum of interband absorption of Ag particles in silica, from the Ag interband dielectric constant [28] and the effective medium permeability [29].

The significant red shift of the absorption edge for the sample with about 1% Ag, with respect to the reference sample, can be mainly attributed to the interband absorption of Ag nanosized particles within pores of silica. From the Ag dielectric constant [28], and correcting for the Drude free electron contribution [28], according to the improved effective medium permeability given by Polder and van Santen [29] (letting the dielectric constant of the silica host be 2.25 [9]), we can obtain the optical absorption spectrum caused by interband absorption of Ag particles in an Ag–silica system, as shown in figure 6 (dashed curve). The detailed calculation and analysis of the shift of the edge will be published elsewhere. We can see that for an Ag-loaded sample with 1 wt% Ag the measured and calculated spectra show good agreement for the edge position.

The significant shift of edge position to lower energy with rising Ag amount can mainly be attributed to the dipole interaction between Ag particles. The distance between Ag particles in silica decreases with increasing Ag amount. When the Ag amount is

sufficiently large, the distance will be small enough that the effective medium theory, which is applied to the situation with independent isolated particles, is invalid and dipole–dipole interaction between particles cannot be disregarded. The reduction of the particles' distance will enhance this interaction. Here we suggest that the interband width of Ag in silica decreases with reduction of the distance between Ag particles due to a complicated, and as yet unknown, interaction between Ag particles, resulting in red shifting of the edge position with rising Ag loading amount. Further investigation of this is in progress.

As to the absence of the plasmon resonance peak in our experiments, further experiments were performed. The doped sample with about 1 wt% Ag was additionally annealed at 1073 K for 1 h. The average diameter of Ag particles is then about 6.3 nm, in contrast to about 2.5 nm for the original treatment. We found that additional annealing induced the apparent plasmon resonance peak at around 400 nm, as shown in figure 6 (curve (e)). A small size of particles will broaden and lower the plasmon resonance peak significantly [30]. There probably exists a quantum size effect in our sample (a quantum size effect will occur when the diameter of the Ag particles is less than 3 nm [25]). Compared with a classical description, the results of a quantum theory calculation [31] show that the surface plasmon mode will be broadened because energy is transferred from the plasmon to single electron excitations between the quantized levels, and reduced in strength by a factor of about two, so the absence of a plasmon resonance peak in our experiments seems to be associated with too small a size of Ag particles in silica. However, the quantum size effect will not cause the suppression of surface plasmon resonance [31]. As previously reported [30, 32], the silver colloids even about 1 nm in diameter still assume plasmon resonances. Under our experimental conditions, interactions at the interface between the pore walls and Ag particles are likely to be extensive, due to the high specific surface area in silica, and the high dispersivity and small size of Ag particles. On this basis, we suggest here that this interface interaction, as yet unknown to us, might act to suppress surface plasmon resonance. When the Ag particles' size is small enough (hence broadening and lowering the plasmon resonance peak) this interaction is relatively large, so as to suppress the plasmon resonance, but when the particle size is larger surface plasmon resonance will become more significant (narrower in width and higher in peak height) and the interface interaction is relatively small, resulting in the appearance of the plasmon resonance peak. However, this aspect, although intuitively reasonable, remains a conjecture with some support from our experiment and needs more detailed investigation.

5. Conclusions

We have successfully assembled mesoporous silica with Ag nanoparticles within its pores by thermal decomposition of $AgNO_3$. The amount of Ag in silica can be controlled by the Ag^+ ion concentration of the soaking solution. The Ag particles are isolated from each other and located within the pores, which are less than 8 nm diameter, and are highly uniformly dispersed. The size distribution of Ag particles can be well fitted by a log-normal distribution function. Ag doping results in a large red shift of the absorption edge which is attributed to the interband absorption of Ag in the Ag–silica system and dipole interaction between Ag particles. In contrast to the extensively reported metal-particle-containing silica (glass), there exists no peak other than the absorption edge for this material, which is, probably, mainly associated with the very small size of Ag particles and an interaction (of a type as yet unclear) at the interfaces between pore walls and Ag particles. Increase of Ag doping amount causes a red shift of the edge across the whole visible region and so the position of the edge is controlled by the doping amount of Ag in silica.

Acknowledgment

The financial support from the National Science Foundation of China is acknowledged.

References

[1] Haperin W P 1986 *Red. Mod. Phys.* **58** 533
[2] Suryanarayana C 1995 *Int. Mater. Rev.* **40**(2) 41
[3] Hudson M and Sequeira C A 1993 *Malfunctional Mesoporous Inorganic Solids* (Dordrecht: Kluwer)
[4] Kresge C T and Leonwicz M E 1992 *Nature* **359** 710
[5] Monnier A 1993 *Science* **261** 1299
[6] Mennig M, Schmitt M, Kutsch B and Schmidt H 1994 *SPIE Proc.* **2288** 120
[7] Judeinstein P and Schmidt H 1994 *J. Sol–Gel Sci. Technol.* **3** 189
[8] Kundu T K and Chakravorty D 1995 *Appl. Phys. Lett.* **66** 3576
[9] Chatterjee A and Chakravorty D 1990 *J. Phys. D: Appl. Phys.* **23** 1097
[10] Zerda T W 1991 *Chemical Processing of Advanced Materials* ed L L Hench and J West (New York)
[11] Rao S, Karaguleff C, Gabel A, Fortenbery R, Seaton C and Stegeman G 1985 *Appl. Phys. Lett.* **46** 801
[12] Wu Chun-Guey and Thomas B 1994 *Science* **264** 1758
[13] Cai Weiping, Tan Ming, Wang Guozhong and Zhang Lide 1996 *Appl. Phys. Lett.* **69** 2980
[14] Cai Weiping, Tan Ming and Zhang Lide 1997 *J. Phys.: Condens. Matter* **9** 1995
[15] Rajh T, Vucemilovic M, Dimitrijevic N, Micic O and Nozik A 1988 *Chem. Phys. Lett.* **49** 1717
[16] Kuczynski J and Thomas J K 1985 *J. Phys. Chem.* **89** 2720
[17] Sato S, Murakata T, Suzuki T and Ohgawara T 1990 *J. Mater. Sci.* **25** 4880
[18] Murakata T, Sato S, Ohgawara T, Natanabe T and Suzuki T 1992 *J. Mater. Sci.* **27** 1567
[19] Ayral A, Phalippou J and Woignier T 1992 *J. Mater. Sci.* **27** 116
[20] Brunauer S, Emmett P H and Teller E 1938 *J. Am. Chem. Soc.* **60** 309
[21] Thomas W 1871 *Phil. Mag.* **42** 448
[22] Wheeler A 1955 *Catalysis* **2** 116
[23] Roy B and Chakravorty D 1990 *J. Phys.: Condens. Matter.* **2** 9323
[24] Forrest S R and Witten T A 1979 *J. Phys. A: Math. Gen.* **12** L109
[25] Kreibig U 1974 *J. Phys. F: Met. Phys.* **4** 999
[26] Cohen R W, Cody G D, Countts M D and Abeles B 1973 *Phys. Rev.* B **8** 3689
[27] Priestley E B, Abeles B and Cohen R W 1975 *Phys. Rev.* B **12** 2121
[28] Johnson P B and Christy R W 1972 *Phys. Rev.* B **6** 4370
[29] Polder D and van Santen J H 1946 *Physica* **12** 257
[30] Mennig M, Spanhel J, Schmidt H and Betzholz S 1992 *J. Non-Cryst. Solids* **147/148** 326
[31] Kawabata A and Kubo R 1966 *J. Phys. Soc. Japan.* **21** 1765
[32] Mennig M 1991 *Mater. Sci. Eng.* B **9** 421